

Limit analysis solutions for the bearing capacity of rock masses using the generalised Hoek–Brown criterion

R.S. Merifield^{a,*}, A.V. Lyamin^b, S.W. Sloan^b

^a*Department of Agricultural, Civil and Environmental Engineering, University of Southern Queensland, QLD 4350, Australia*

^b*Department of Civil, Surveying and Environmental Engineering, The University of Newcastle, NSW 2308, Australia*

Accepted 3 February 2006

Available online 31 March 2006

Abstract

This paper applies numerical limit analyses to evaluate the ultimate bearing capacity of a surface footing resting on a rock mass whose strength can be described by the generalised Hoek–Brown failure criterion [Hoek E, Carranza-Torres C, Corkum B. Hoek–Brown failure criterion—2002 edition. In: Proceedings of the North American rock mechanics society meeting in Toronto, 2002]. This criterion is applicable to intact rock or heavily jointed rock masses that can be considered homogeneous and isotropic. Rigorous bounds on the ultimate bearing capacity are obtained by employing finite elements in conjunction with the upper and lower bound limit theorems of classical plasticity. Results from the limit theorems are found to bracket the true collapse load to within approximately 2%, and have been presented in the form of bearing capacity factors for a range of material properties. Where possible, a comparison is made between existing numerical analyses, empirical and semi-empirical solutions.

© 2006 Elsevier Ltd. All rights reserved.

Keywords: Bearing capacity; Rock; Failure; Footings/foundations; Numerical modelling

1. Introduction

The ultimate bearing capacity is an important design consideration for dams, roads, bridges and other engineering structures, particularly when large rock masses are the foundation materials. With the exception of some very soft rocks and heavily jointed media, the majority of rock masses provide an excellent foundation material. However, there is a need to accurately estimate the ultimate bearing capacity for structures with high foundation loads such as tall buildings and dams.

Rigorous theoretical solutions to the problem of foundations resting on rock masses do not appear to exist in the literature. This may be attributed to the fact that rock masses are inhomogeneous, discontinuous media composed of rock material and naturally occurring discontinuities such as joints, fractures and bedding planes.

This makes the derivation of simple theoretical solutions based on limit equilibrium methods very difficult. In addition, fractures and discontinuities occurring naturally in rock masses are difficult to model using the displacement finite element method without the addition of special interface or joint elements. The upper and lower bound formulations of Lyamin and Sloan [1,2] are ideally suited to analysing jointed or fissured materials due to the existence of discontinuities throughout the mesh. These discontinuities allow an abrupt change in stresses in the lower bound formulation and in velocities in the upper bound formulation. Moreover, employing discontinuities when modelling geotechnical problems enables great flexibility as they can be assigned different material properties and/or yield criteria. This unique feature was recently exploited by Sutcliffe et al. [3] and Zheng et al. [4] who used the formulations of Sloan [5] and Sloan and Kleeman [6] to analyse the bearing capacity of jointed rock and fissured materials respectively.

The purpose of this paper is to take advantage of the ability of the limit theorems to bracket the actual collapse load by computing both lower and upper bounds for the

*Corresponding author. Tel.: +61 746 311 325; fax: +61 746 312 526.

E-mail addresses: richard.merifield@usq.edu.au (R.S. Merifield), andrei.lyamin@newcastle.edu.au (A.V. Lyamin), scott.sloan@newcastle.edu.au (S.W. Sloan).

bearing capacity of strip footings on a broken rock mass. These solutions are obtained using the numerical techniques developed by Lyamin and Sloan [1,2] which have been modified to incorporate the well-known Hoek–Brown yield criterion [7]. The applicability and background of the Hoek–Brown criterion will be discussed in the following section in more detail.

2. The generalised Hoek–Brown failure criterion

2.1. Applicability

It is well known that the strength of jointed rock masses is notoriously difficult to assess. The behaviour of a rock mass is complicated greatly because deformations and sliding along naturally occurring discontinuities can occur in addition to deformations and failure in the intact parts (blocks) of the rock mass. Unfortunately, laboratory tests on specific core samples is often not representative of a rock mass at field scale, while in situ strength testing of the rock mass is seldom practically or economically feasible. Nonetheless, engineers and geologists are required to predict the strength of large-scale rock masses when designing such things as drifts, foundations, slopes, tunnels and caverns.

Many criteria have been developed that seek to capture the important elements of measured rock strength or seek to modify theoretical approaches to accommodate experimental evidence. One currently accepted approach to estimating rock mass strength is to use the Hoek–Brown failure criterion where the required parameters are estimated with the help of a rock mass classification system. The Hoek–Brown failure criterion is an empirical criterion developed through curve-fitting of triaxial test data. It was originally developed in the 1980s [8] for intact rock and jointed rock masses, and has been subject to continual refinement [7]. The Hoek–Brown criterion is one of the few non-linear criteria used by practising engineers [9] to estimate rock mass strength. It is therefore appropriate to use this yield criterion when predicting the bearing capacity of surface foundations on rock.

It is important to note that the Hoek–Brown failure criterion, which assumes isotropic rock and rock mass behaviour, should only be applied to those rock masses in which there are a sufficient number of closely spaced discontinuities, with similar surface characteristics, that isotropic behaviour involving failure on discontinuities can be assumed. When the structure being analysed is large and the block size small in comparison, the rock mass can be treated as a Hoek–Brown material. Where the block size is of the same order as that of the structure being analysed, or when one of the discontinuity sets is significantly weaker than the others, the Hoek–Brown criterion should not be used. In these cases, the stability of the structure should be analysed by considering failure mechanisms involving the sliding or rotation of blocks and wedges defined by intersecting structural features.

With reference to the bearing capacity problem considered herein, the applicability of the Hoek–Brown criterion is best described by referring to Fig. 1. After Hoek [10] it appears three main structural groups can be differentiated for rock masses, namely GROUP I, GROUP II, and GROUP III. Fig. 1 shows the transition from an isotropic intact rock (GROUP I), through a highly anisotropic rock mass (GROUP II), to an isotropic heavily jointed rock mass (GROUP III), with increasing sample size for a surface foundation on a hypothetical rock mass. Which of these structural groups will apply in a given case will depend on the width of the foundation relative to the discontinuity spacing, and the orientations and strengths of the discontinuities. In this paper it has been assumed that the underlying rock mass is either: (1) intact or; (2) heavily jointed with “small spacing” between discontinuities so that, on the scale of the problem, it can be regarded as an isotropic assembly of interlocking particles. Consequently, the results presented are valid for “intact rock” (GROUP I) and “several discontinuities” and “jointed rock mass” (GROUP III) conditions, respectively.

The relative concept of “small spacing” as mentioned above, was proposed by Serrano and Olalla [11] as a means of quantifying the validity of using the Hoek–Brown failure criterion for bearing capacity predictions. A new parameter, the “spacing ratio of a foundation” (*SR*) was proposed that depends, among other things, on the width of the foundation. It is defined by the expression;

$$SR = B \sum_{i=1}^n \frac{1}{S_{mi}} = B \sum_{i=1}^n \lambda_i,$$

where *B* is the foundation width; *S_{mi}* is the joint spacing of the *i*th discontinuity family; *λ_i* is the frequency of the *i*th discontinuity family; and *n* is the number of discontinuity families. Serrano and Olalla suggest a relatively “small spacing” is when (*SR*) is greater than 60. This would imply that there are four families of discontinuities each appearing 15 times across the foundation width. Therefore the Hoek–Brown criterion is not valid when *SR* < 60, except when the value of *SR* is so low that the rock mass can be considered as intact and belonging to the aforementioned GROUP I.

It should be noted that, in the case of intact rock (GROUP I), common sense needs to be exercised when using the results presented in this paper since the failure of the foundation may be brittle rather than plastic.

The effect of scale on the bearing capacity of foundations on rock needs to be considered, particularly when the underlying assumption is that the rock mass behaves as a homogeneous isotropic continuous medium. There will be a distinct difference in the ultimate behaviour of “large” and “small” foundations. For the case of “large” foundations where the load covers an extensive area, a considerable volume of the rock mass is affected and the stresses caused by gravity on the potential flow surfaces are comparable to that part of the strength which is due to

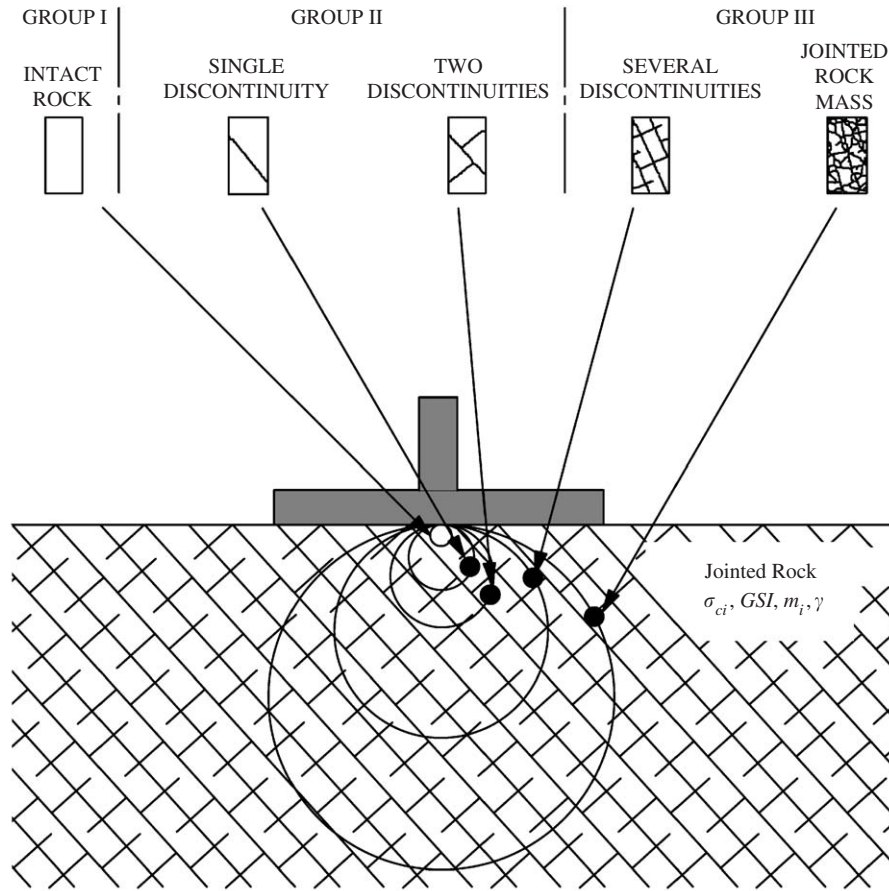


Fig. 1. Applicability of the Hoek–Brown yield criterion for shallow foundations.

the rock cohesion. In this case it seems reasonable to assume that such a problem can be studied using plasticity theories. However, “small” foundations only influence a small volume of the rock mass and the stresses caused by self-weight will be negligible when compared to the strength of the rock. In this case the ultimate behaviour may be brittle in nature and the theories of plasticity may not be appropriate. Unfortunately, there is currently no guidance for engineers regarding what constitutes a “large” or “small” foundation. As pointed out by Serrano and Olalla [11] more research is required to quantify this problem.

2.2. Limit analysis implementation

One of the key features of the Lyamin and Sloan [1,2] formulations is that they can deal with general yield criteria including multi-surface ones where several convex domains are combined to constrain the stresses at each node of the mesh. These combinations can be different for different parts of the discretised body. Because they are employed in their native form, a wide range of yield criteria can be used in the analysis. Each of the surfaces must be convex and smooth but the resulting composite surface, though convex, is generally non-smooth. An example of a multi-surface yield function is where the conventional (non-

smooth) Tresca criterion is combined with a transition surface to round the corners in the octahedral plane. Another example is the use of a simple plane to cut the apex of a cone-like yield surface. This type of cut-off is often used for modelling materials such as rock, and leads to a cup-shaped surface.

In this section, details of the latest version of the Hoek–Brown yield criterion [7] and how it has been incorporated into the limit analysis formulations of Lyamin and Sloan [1,2] are discussed.

The Hoek–Brown failure criterion for rock masses was first described in 1980 [8] and has been subsequently updated in 1983, 1988, 1992, 1995, 1997, 2001 and 2002. A brief history of its development can be found in Hoek [12]. The latest version that is used here can be written as

$$\sigma'_1 = \sigma'_3 + \sigma_{ci} \left(m_b \frac{\sigma'_3}{\sigma'_{ci}} + s \right)^\alpha \tag{1}$$

The relationships between m_b/m_i , s and α and the geological strength index (GSI) are as follows:

$$m_b = m_i \exp\left(\frac{GSI - 100}{28 - 14D}\right), \tag{2}$$

$$s = \exp\left(\frac{GSI - 100}{9 - 3D}\right), \tag{3}$$

$$\alpha = \frac{1}{2} + \frac{1}{6} \left(e^{-GSI/15} - e^{-20/3} \right). \quad (4)$$

The *GSI* was introduced because Bieniawski’s rock mass rating (*RMR*) system [13] and the *Q*-system [14] were deemed to be unsuitable for poor rock masses. The *GSI* ranges from about 10, for extremely poor rock masses, to 100 for intact rock. The parameter *D* is a factor that depends on the degree of disturbance. The suggested value of the disturbance factor is *D* = 0 for undisturbed in situ rock masses and *D* = 1 for disturbed rock mass properties. For the analyses presented here, a value of *D* = 0 has been adopted.

The unconfined compressive strength is obtained by setting $\sigma_3 = 0$ in Eq. (1), giving

$$\sigma_c = \sigma_{ci} s^\alpha \quad (5)$$

and the tensile strength is

$$\sigma_t = -\frac{s\sigma_{ci}}{m_b}. \quad (6)$$

In a similar manner to the Mohr–Coulomb failure envelope, the Hoek–Brown yield surface has apex and corner singularities in stress space. The direct computation of the derivatives at these locations, which are required for

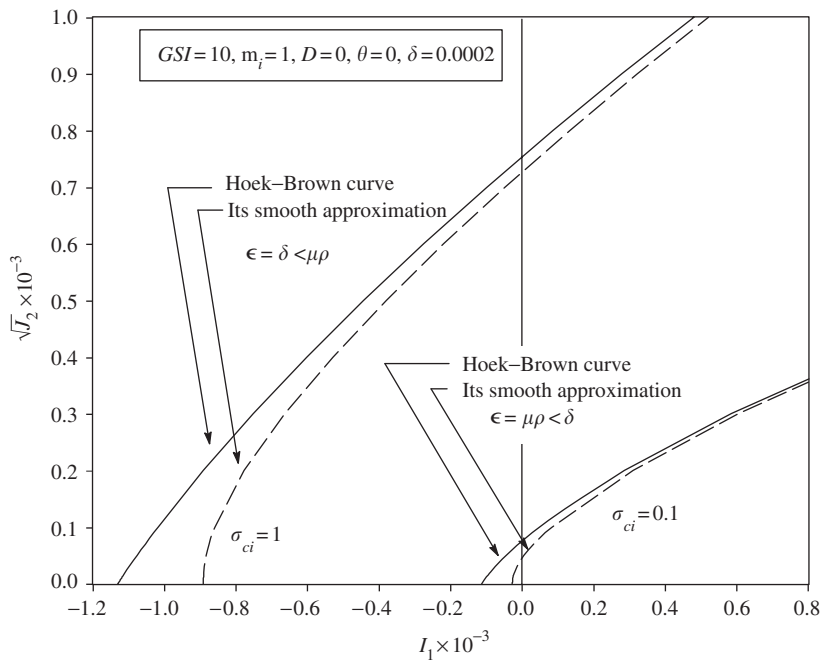


Fig. 2. Meridian plane section of Hoek–Brown yield surface and its smooth approximation.

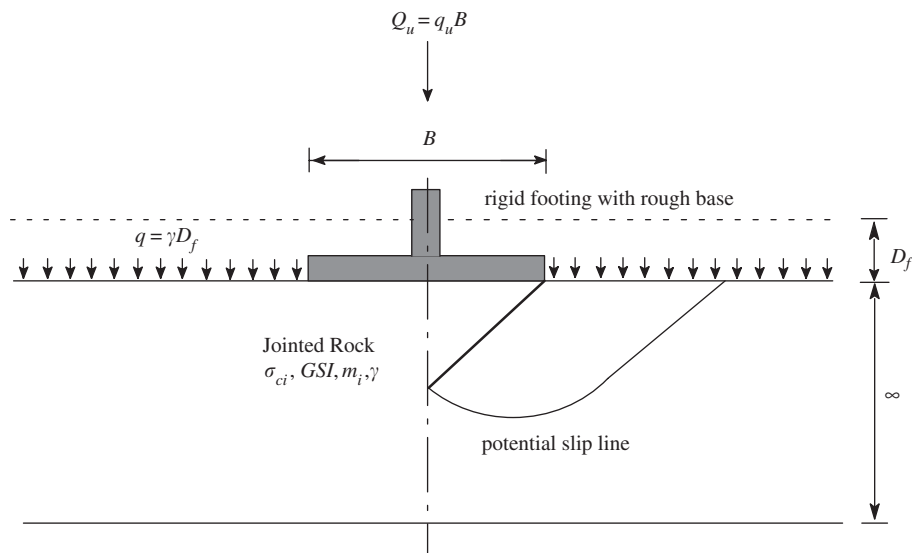


Fig. 3. Problem definition.

the non-linear programming (NLP) solver, becomes impossible. This issue can be resolved using three different approaches; namely, global smoothing, local smoothing and multi-surface representation (which includes both a priori and dynamic linearisation). As the current study is limited to the case of plain strain conditions, the corners are automatically avoided and the only singularity which needs to be dealt with is the apex of the yield surface. The easiest options to implement are a simple tension cut-off (which is a multi-surface technique) or a quasi-

hyperbolic approximation (which is a global smoothing technique). The authors decided to adopt the later approach as a similar method has been previously employed by Abbo and Sloan [15] for smoothing the Mohr–Coulomb yield criteria. The prefix “quasi” is used here because the Hoek–Brown yield surface is already curved in the meridional plane and the suggested approximation is not a pure hyperbolic one. A brief description of the procedure is provided as follows (more details can be found in [15]).

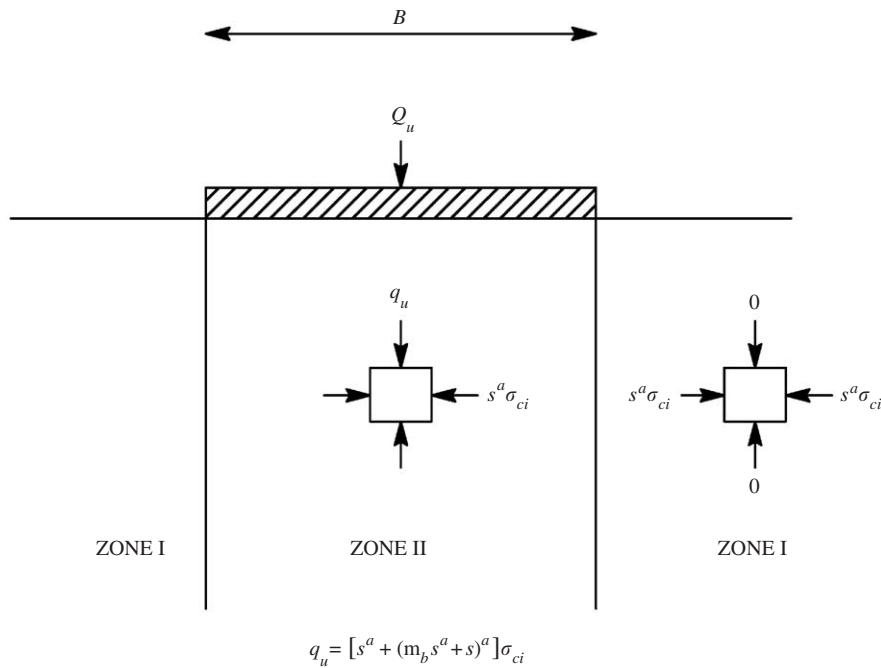


Fig. 4. Lower bound solution for bearing capacity (after Kulhawy and Carter [20]).

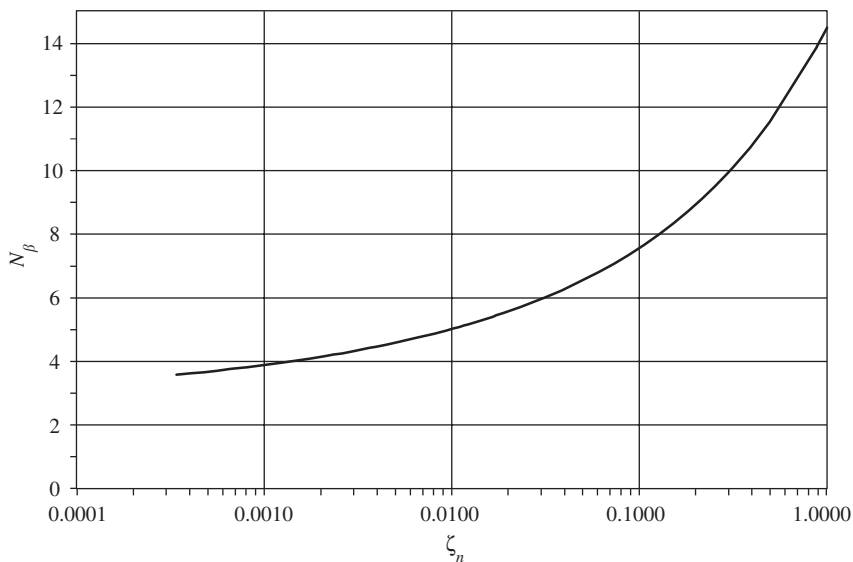


Fig. 5. Bearing capacity factor for weightless rock (after Serrano et al. [24]).

First, the Hoek–Brown yield function given in Eq. (1) is expressed in terms of stress invariants as

$$f_{\text{HB}} = \sqrt{J_2}g(\theta) + \left(\sqrt{J_2}h(\theta) + \beta I_1 + \chi \right)^\alpha, \quad (7)$$

where I_1 is the first stress invariant, J_2 is the second deviatoric stress invariant and θ is the Lode angle related to the third deviatoric stress invariant J_3 , whereas parameters β and χ , and functions $g(\theta)$ and $h(\theta)$ are given by the following expressions:

$$g(\theta) = -2 \cos(\theta), \quad (8)$$

$$h(\theta) = -m_b \sigma_{ci}^{(1-\alpha)/\alpha} \left(\cos(\theta) + \frac{\sin(\theta)}{\sqrt{3}} \right), \quad (9)$$

$$\beta = m_b \sigma_{ci}^{(1-\alpha)/\alpha}, \quad (10)$$

$$\chi = s \sigma_{ci}^{1/\alpha}. \quad (11)$$

Next, quasi-hyperbolic smoothing is applied by permuting J_2 with a small term ε according to

$$\hat{J}_2 = \sqrt{J_2 + \varepsilon^2}, \quad (12)$$

on condition that ε is related to the tensile strength of material by the rule

$$\varepsilon = \min(\delta, \mu \rho | \rho g(0) + (\rho h(0) + \chi)^\alpha = 0). \quad (13)$$

The constants δ and μ must be chosen to balance the efficiency of the NLP solver against the accuracy of the

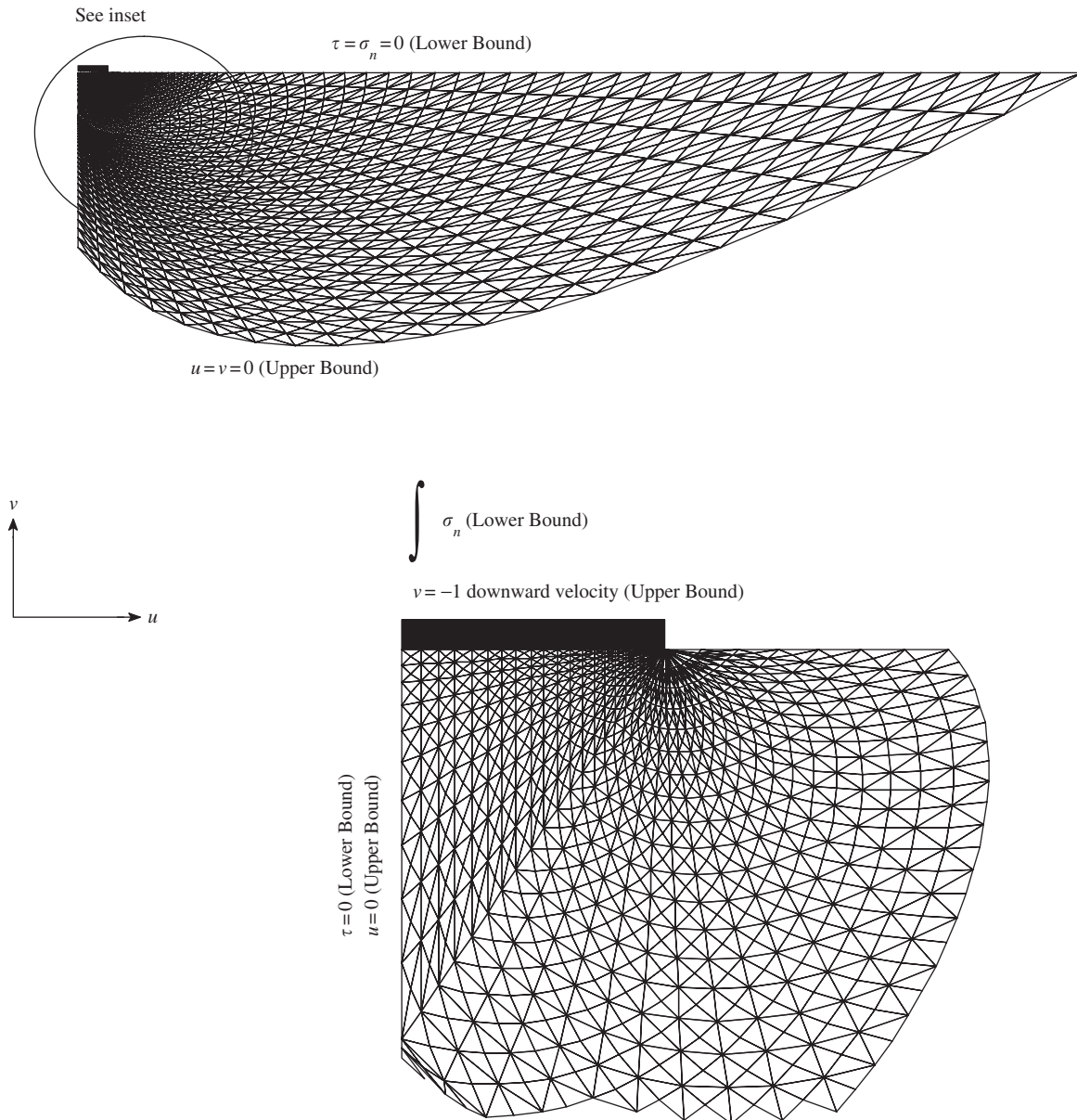


Fig. 6. Typical finite element mesh.

representation of the original yield surface. The values used in the current study are $\delta = 10^{-6}$ and $\mu = 10^{-1}$.

The resulting approximation of the Hoek–Brown yield criterion can be written as

$$f_{HB} = \hat{J}_2 g(\theta) + (\hat{J}_2 h(\theta) + \beta I_1 + \chi)^\alpha \tag{14}$$

and is now a smooth and convex function in the meridional plane. An illustration of the original and smoothed Hoek–Brown curves in the $(I_1, \sqrt{J_2})$ plane for zero θ is given in Fig. 2. It should be noted that the difference between the smooth approximation and the original yield surface has been greatly exaggerated in this figure by selecting values of μ and ρ that are much larger than what was actually adopted. The original and smoothed yield surfaces are almost indistinguishable when the actual values of μ and ρ are used.

2.3. Equivalent Mohr–Coulomb parameters

Since many geotechnical analysis methods still use the Mohr–Coulomb failure criterion, it is sometimes necessary for practising engineers to determine equivalent angles of friction and cohesive strengths for each rock mass and stress range. In the context of this paper, estimating these equivalent parameters will enable a direct comparison to be

made between Hoek–Brown solutions and equivalent Mohr–Coulomb solutions.

The choice of method to use for determining equivalent cohesion and friction angle is largely a matter of taste and experience. An equivalent cohesion and friction angle at a specified normal stress or minor principal stress, as determined by an elastic analysis, may give locally accurate values for a small stress variation. Alternatively, average values applicable to a wider range of stress conditions may be obtained by using a regression procedure. However, this may lead to an underestimate of the strength for low stresses and an overestimate for high stresses. Nonetheless, a regression approach appears to be the most widely accepted method and is typically performed by fitting a linear relationship to the curve generated by Eq. (1) for a range of minor principal stress values defined by $\sigma_t < \sigma_3 < \sigma_{3\max}$. This has been performed recently by Hoek et al. [7] where the fitting process involves balancing the areas above and below the Mohr–Coulomb relation. This results in the following equations for the angle of friction and cohesive strength:

$$c' = \frac{\sigma_{ci}[(1 + 2\alpha)s + (1 - \alpha)m_b\sigma'_{3n}](s + m_b\sigma'_{3n})^{\alpha-1}}{(1 + \alpha)(2 + \alpha)\sqrt{1 + (6\alpha m_b(s + m_b\sigma'_{3n})^{\alpha-1})/(1 + \alpha)(2 + \alpha)}}, \tag{15}$$

Table 1
Values of the bearing capacity factor for a weightless rock

<i>GSI</i>	<i>m_i</i>	<i>N_{σ0}</i> Average	<i>N_{σ0}</i> Kulhawy and Carter [20]	<i>N_{σ0}</i> Serrano et al. [24]	<i>GSI</i>	<i>m_i</i>	<i>N_{σ0}</i> Average	<i>N_{σ0}</i> Kulhawy and Carter [20]	<i>N_{σ0}</i> Serrano et al. [24]
10	1	0.015	0.009 (−40%)	0.010 (−35%)	60	1	0.465	0.299 (−36%)	0.458 (−1%)
10	5	0.042	0.016 (−61%)	0.035 (−17%)	60	5	1.013	0.479 (−53%)	1.006 (−1%)
10	10	0.077	0.022 (−71%)	0.072 (−7%)	60	10	1.597	0.623 (−61%)	1.588 (−1%)
10	20	0.156	0.032 (−80%)	0.159 (+2%)	60	20	2.667	0.830 (−69%)	2.658 (0%)
10	30	0.238	0.039 (−83%)	0.259 (+9%)	60	30	3.644	0.990 (−73%)	3.673 (+1%)
10	35	0.288	0.043 (−85%)	0.314 (+9%)	60	35	4.186	1.060 (−75%)	4.170 (0%)
20	1	0.044	0.026 (−41%)	0.036 (−16%)	70	1	0.765	0.503 (−34%)	0.759 (−1%)
20	5	0.119	0.046 (−61%)	0.111 (−6%)	70	5	1.582	0.785 (−50%)	1.574 (−1%)
20	10	0.209	0.062 (−70%)	0.204 (−2%)	70	10	2.444	1.012 (−59%)	2.434 (0%)
20	20	0.389	0.086 (−78%)	0.397 (+2%)	70	20	4.012	1.339 (−67%)	3.998 (0%)
20	30	0.575	0.106 (−82%)	0.600 (+4%)	70	30	5.491	1.592 (−71%)	5.470 (0%)
20	35	0.670	0.114 (−83%)	0.704 (+5%)	70	35	6.068	1.703 (−72%)	6.187 (+2%)
30	1	0.092	0.054 (−41%)	0.084 (−8%)	80	1	1.260	0.847 (−33%)	1.254 (−1%)
30	5	0.235	0.095 (−60%)	0.227 (−3%)	80	5	2.473	1.284 (−48%)	2.463 (0%)
30	10	0.397	0.127 (−68%)	0.393 (−1%)	80	10	3.745	1.640 (−56%)	3.732 (0%)
30	20	0.713	0.174 (−76%)	0.716 (0%)	80	20	6.040	2.154 (−64%)	6.019 (0%)
30	30	1.022	0.210 (−79%)	1.038 (+2%)	80	30	8.195	2.553 (−69%)	8.171 (0%)
30	35	1.193	0.226 (−81%)	1.200 (+1%)	80	35	9.242	2.727 (−70%)	9.210 (0%)
40	1	0.165	0.101 (−39%)	0.158 (−4%)	90	1	2.083	1.428 (−31%)	2.076 (0%)
40	5	0.401	0.171 (−57%)	0.393 (−2%)	90	5	3.881	2.102 (−46%)	3.869 (0%)
40	10	0.659	0.226 (−66%)	0.654 (−1%)	90	10	5.758	2.658 (−54%)	5.741 (0%)
40	20	1.149	0.306 (−73%)	1.147 (0%)	90	20	9.125	3.466 (−62%)	9.100 (0%)
40	30	1.630	0.368 (−77%)	1.626 (0%)	90	30	12.270	4.092 (−67%)	12.237 (0%)
40	35	1.873	0.395 (−79%)	1.863 (−1%)	90	35	13.794	4.367 (−68%)	13.738 (0%)
50	1	0.281	0.176 (−37%)	0.274 (−3%)	100	1	3.461	2.414 (−30%)	3.449 (0%)
50	5	0.644	0.290 (−55%)	0.638 (−1%)	100	5	6.124	3.449 (−44%)	6.114 (0%)
50	10	1.037	0.380 (−63%)	1.031 (−1%)	100	10	8.896	4.317 (−51%)	8.875 (0%)
50	20	1.765	0.510 (−71%)	1.760 (0%)	100	20	13.847	5.583 (−60%)	13.809 (0%)
50	30	2.467	0.610 (−75%)	2.458 (0%)	100	30	18.444	6.568 (−64%)	18.390 (0%)
50	35	2.817	0.654 (−77%)	2.801 (−1%)	100	35	20.668	7.000 (−66%)	20.628 (0%)

$$\phi' = \sin^{-1} \left[\frac{6\alpha m_b (s + m_b \sigma'_{3n})^{\alpha-1}}{2(1 + \alpha)(2 + \alpha) + 6\alpha m_b (s + m_b \sigma'_{3n})^{\alpha-1}} \right], \quad (16)$$

where $\sigma_{3n} = \sigma'_{3\max} / \sigma_{ci}$.

Note that the value of $\sigma'_{3\max}$, the upper limit of confining stress over which the relationship between the Hoek–Brown and the Mohr–Coulomb criteria is considered, has to be determined for each individual case. Of course it is likely that the stresses will vary greatly throughout the rock mass which will make it difficult to select a representative value of $\sigma'_{3\max}$. As far as the authors are aware, there are no theoretically correct methods for choosing this range and a trial and error method, based upon practical compromise, is

suggested by Hoek [16]. From experience and trial and error, Hoek and Brown [17] suggest a value of $\sigma'_{3\max} = 0.25\sigma_{ci}$ will provide consistent results. More specific guidance is provided by Hoek [16] for selecting appropriate values of $\sigma'_{3\max}$ specifically for tunnels and slopes. However, no guidance is provided for the case of a surface footing.

3. Problem definition

The plane strain bearing capacity problem to be considered is illustrated in Fig. 3. A strip footing of width B rests upon a jointed rock mass with an intact uniaxial compressive strength σ_{ci} , geological strength index GSI ,

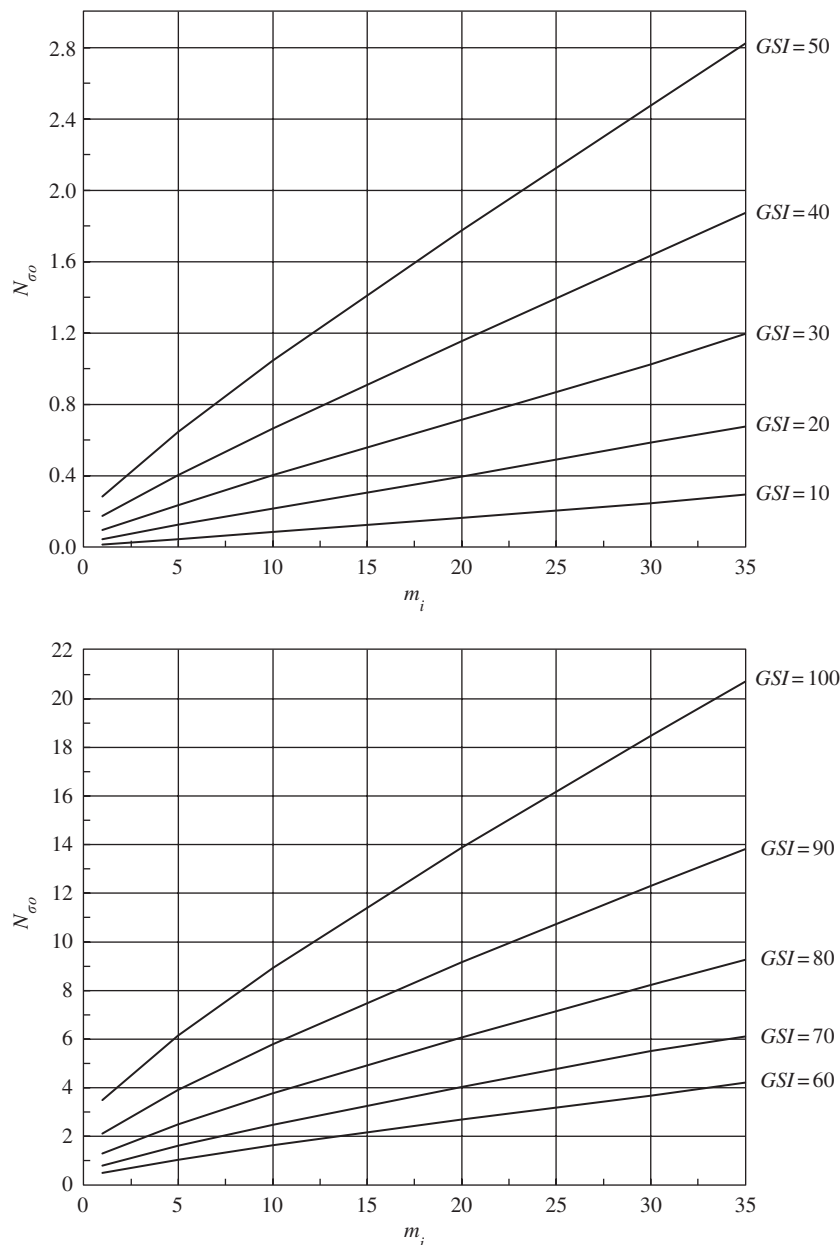


Fig. 7. Bearing capacity factor for weightless rock.

rock mass unit weight γ , and intact rock yield parameter m_i . The ultimate capacity can be written as

$$q_u = \sigma_{ci} N_\sigma, \tag{17}$$

where N_σ is defined as the bearing capacity factor. For a weightless rock mass ($\gamma = 0$), the above expression is valid but the bearing capacity factor N_σ is replaced with $N_{\sigma 0}$. The form of Eq. (17) is a convenient way of expressing the ultimate bearing capacity as a “fraction” of the uniaxial compressive strength and is historically consistent with previous bearing capacity representations.

In the following, the ultimate bearing capacity will be estimated for a practical range of GSI , γ and m_i values.

4. Previous studies

A review of the literature reveals that very few thorough numerical analyses have been performed to determine the ultimate bearing capacity of shallow foundations on rock. Of the numerical studies that have been presented, few can be considered as rigorous. The ultimate tip bearing capacity of pile foundations, on the other hand, has

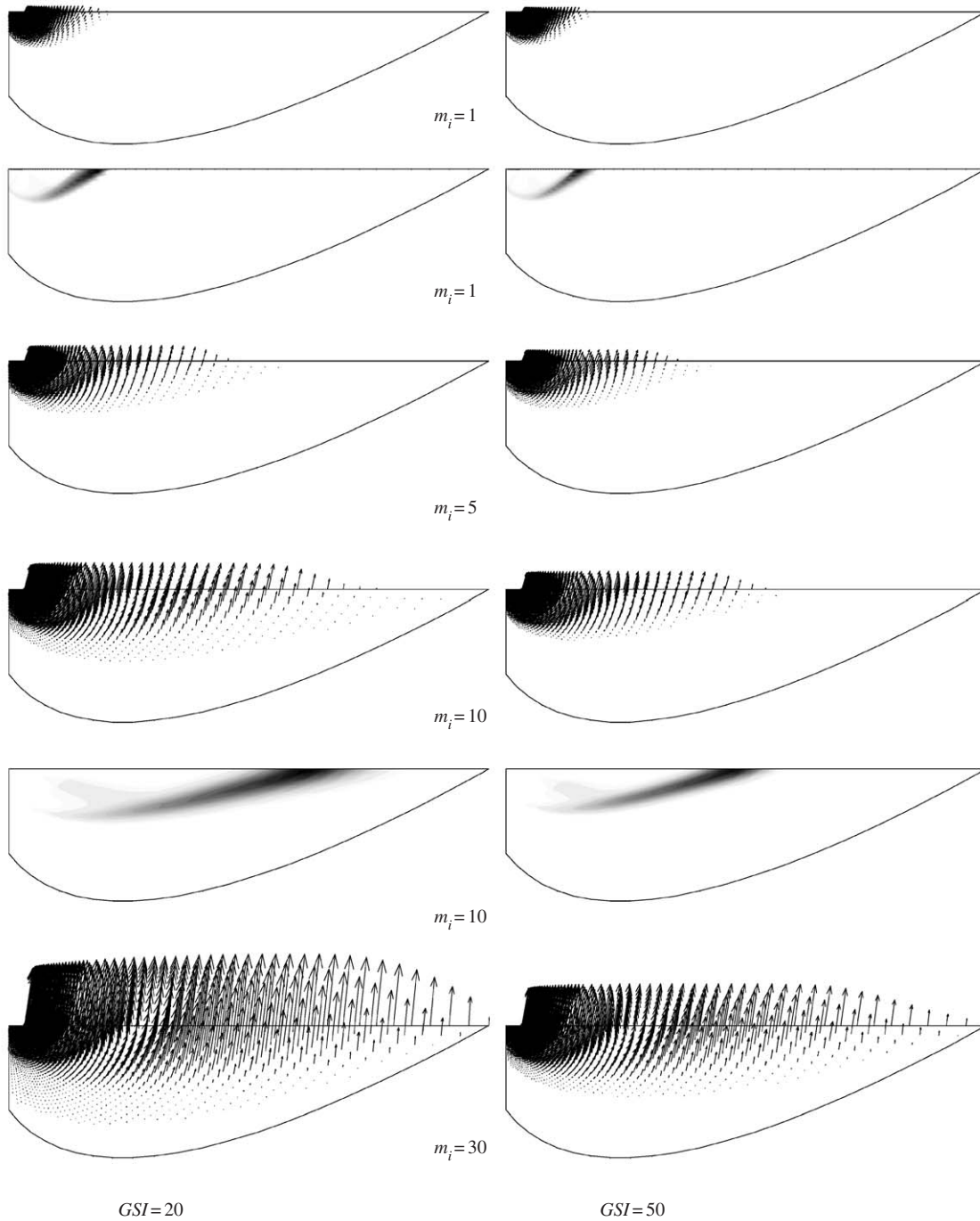


Fig. 8. Upper bound velocity fields and plastic zones for weightless rock.

received much more attention and is discussed by Serrano and Olalla [11,18].

Carter and Kulhawy [19] and Kulhawy and Carter [20] proposed a simple lower bound solution for the bearing capacity of a weightless rock mass obeying a non-linear Hoek–Brown yield criterion. The details of the lower bound stress field are shown in Fig. 4. A lower bound to the failure load q_u is calculated by finding a stress field that satisfies both equilibrium and the failure criterion. The rock mass beneath the strip footing is divided into two zones as shown. The vertical stress σ_3 in zone I is assumed to be zero (weightless), while the horizontal stress (σ_1) is equal to the unconfined compressive strength of the rock mass, as given by Eq. (5). For equilibrium, continuity of

the normal stress across the discontinuity between the zones must be maintained. The bearing capacity of the strip footing may thus be evaluated from Eq. (1) (with $\sigma_3 = s^\alpha \sigma_{ci}$) as

$$q_u = [s^\alpha + (m_b s^\alpha + s)^\alpha] \sigma_{ci}, \tag{18}$$

which to be consistent with Eq. (17) can be written as

$$q_u = N_{\sigma 0} \sigma_{ci},$$

where

$$N_{\sigma 0} = [s^\alpha + (m_b s^\alpha + s)^\alpha] \tag{19}$$

is the bearing capacity factor for a weightless rock mass as defined previously.

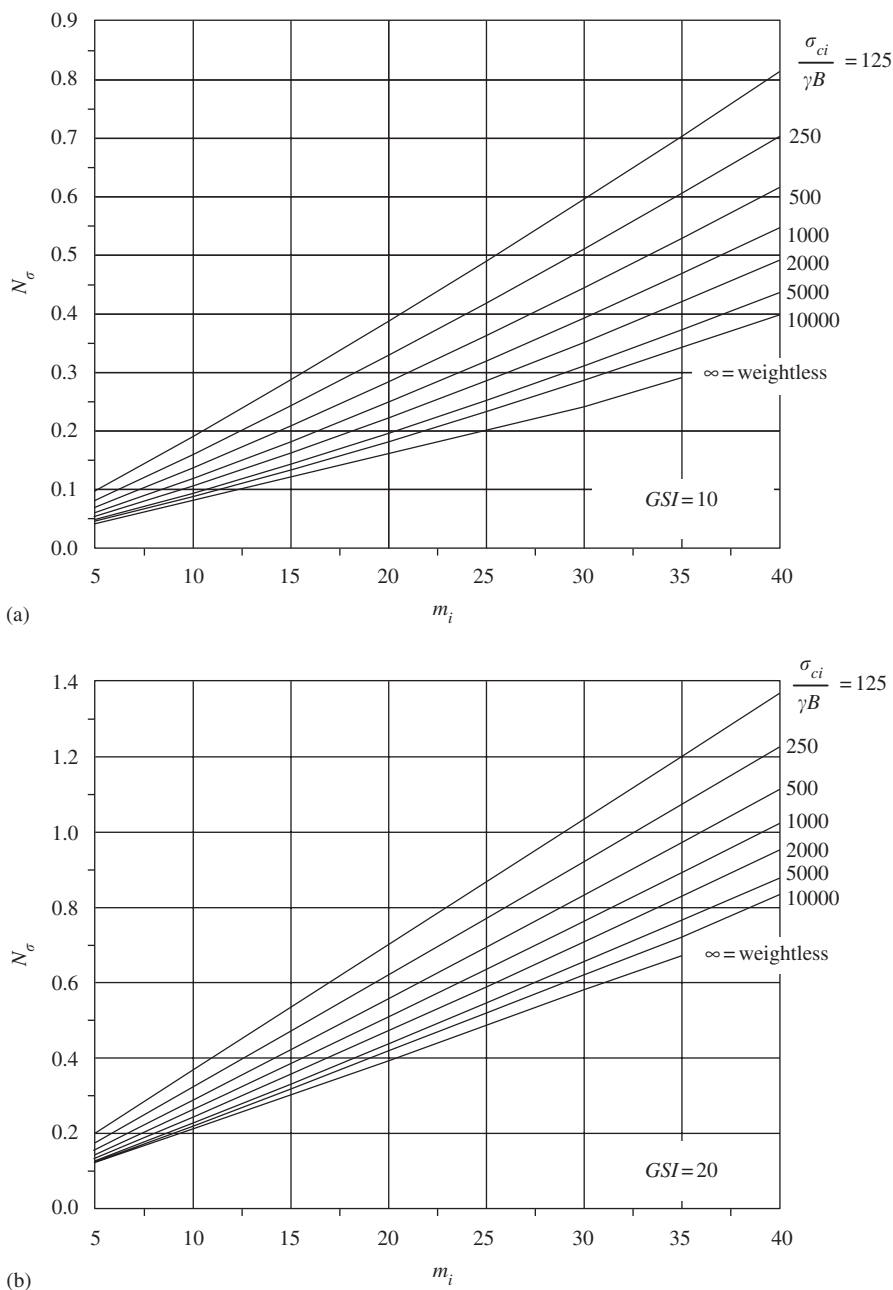


Fig. 9. Average finite element limit analysis values of the bearing capacity factor N_σ .

Eq. (18), along with the categories of rock type and rock mass condition presented by Hoek [10], have been used to produce guidelines for estimating the bearing capacity of rock masses [21].

Serrano and Olalla [22,23] and Serrano et al. [24] proposed a method for estimating the ultimate bearing capacity for a strip footing on a weightless rock mass with or without a surface surcharge. The method is based upon the slip-line method developed by Sokolovskii [25].

The ultimate bearing capacity q_u , as proposed by Serrano et al. [24] using the Hoek–Brown criterion presented by Hoek et al. [26], is expressed as

$$q_u = P_h = \beta_n(N_\beta - \zeta_n), \tag{20}$$

where ζ_n and β_n are constants for the rock mass and depend on m_b , α , s and σ_{ci} according to

$$A_n = \left(\frac{m_b(1-\alpha)}{2^{1/\alpha}} \right)^{\alpha/(1-\alpha)}, \quad \beta_n = A_n \sigma_{ci}, \quad \zeta_n = \frac{s}{m_b A_n}.$$

ζ_n is referred to as the “rock mass toughness” while β_n is referred to as the “strength modulus” [27,28]. N_β is a function of the normalised external load on the boundary adjacent to the footing. If there is no surface surcharge on this boundary, then N_β can be determined using the method outlined by Serrano and Olalla [22] and is shown graphically in Fig. 5. Note that this figure has been produced using the most recent version of the Hoek–Brown yield criterion, and not the earlier version [26] used in the paper by Serrano et al. [24].

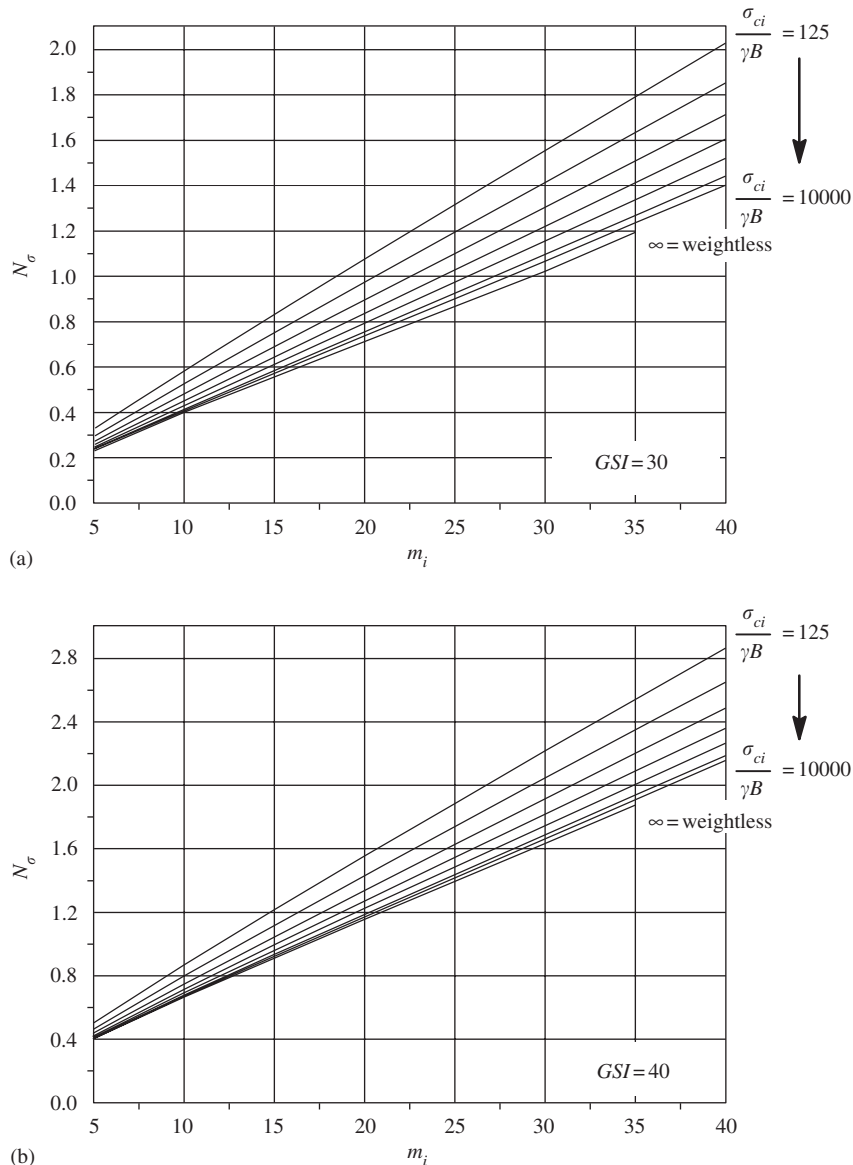


Fig. 10. Average finite element limit analysis values of the bearing capacity factor N_σ .

More recently, Xiaoli et al. [29] formulated an analytical lower bound for the bearing capacity of a strip footing resting on a Hoek–Brown material. Very few results, however, were presented.

5. Results and discussion

The computed upper and lower bound estimates of the bearing capacity factor N_σ for both the weightless and ponderable rock analyses were found to be within 5% of each other. This indicates that, for practical design purposes, the true collapse load has been bracketed to within $\pm 2.5\%$ or better. As a consequence, average values of the upper and lower bound bearing capacity factor have been calculated and will be used in the following discussions.

Typical upper and lower bound meshes for the problem, along with the applied stress and velocity boundary

conditions, are shown in Fig. 6. The results presented are for the case of a perfectly rough rigid footing. For the lower bound, this boundary condition is achieved by assuming the individual normal stresses at element nodes on the soil/footing interface are unrestricted in magnitude. In the upper bound case, a uniform velocity is prescribed for all the nodes along the footing. The overall upper bound and lower bound mesh dimensions were selected such that they adequately contained all plastic zones.

5.1. Weightless rock masses

For the weightless rock case the bearing capacity factor has been defined as $N_{\sigma 0}$. The average upper and lower bound estimates of $N_{\sigma 0}$ are summarised in Table 1 and Fig. 7 for a range of GSI and m_i values. As expected, for a given GSI , increasing m_i leads to an increase in the ultimate

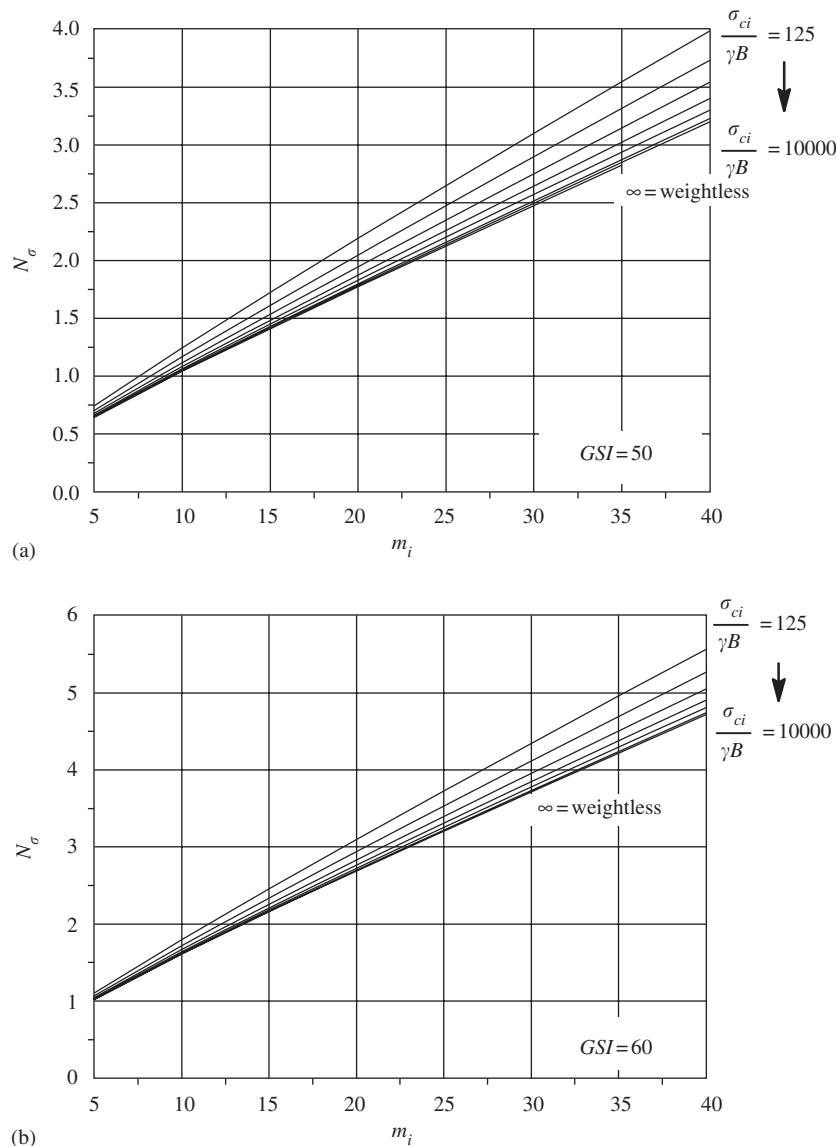


Fig. 11. Average finite element limit analysis values of the bearing capacity factor N_σ .

bearing capacity. Fig. 7 indicates that $N_{\sigma 0}$ increases non-linearly with m_i and GSI .

Fig. 8 presents several of the observed upper bound velocity fields and plastic zones. For a given GSI , as m_i increases, so does the extent of the observed velocity field and zone of plastic yielding. This is expected as an increase in m_i will, in essence, increase the strength of the rock and the equivalent Mohr–Coulomb parameters. Interestingly the same effect is not observed when, for a given m_i , an increase in GSI leads to a reduction in the extent of both the velocity field and zone of plastic shearing.

5.2. Rock masses with unit weight

The effect of rock weight and rock strength has been incorporated in the analyses using the non-dimensional

factor $\sigma_{ci}/\gamma B$ which varies between 125 and 10000. This range will cover most problems of practical interest.

The average upper and lower bound estimates of the bearing capacity factor N_{σ} are summarised in Figs. 9–12 for a range of GSI and m_i values. For a given GSI , increasing m_i leads to an almost linear increase in the bearing capacity factor N_{σ} .

Referring to the above figures, the effects of including self-weight in the analyses may be explained as follows. For any given rock mass (σ_{ci}, GSI, m_i) and foundation width B (i.e. $\sigma_{ci}/B = \text{constant}$), the addition of self-weight γ (i.e. decrease in the ratio $\sigma_{ci}/\gamma B$) will lead to an increase in the bearing capacity factor N_{σ} and thus the ultimate bearing capacity. That is, the bearing capacity factor for a weightless rock $N_{\sigma 0}$ is always less than the bearing capacity factor N_{σ} for a rock with unit weight ($N_{\sigma} \geq N_{\sigma 0}$). The effect of a small increase or decrease in the estimated rock weight

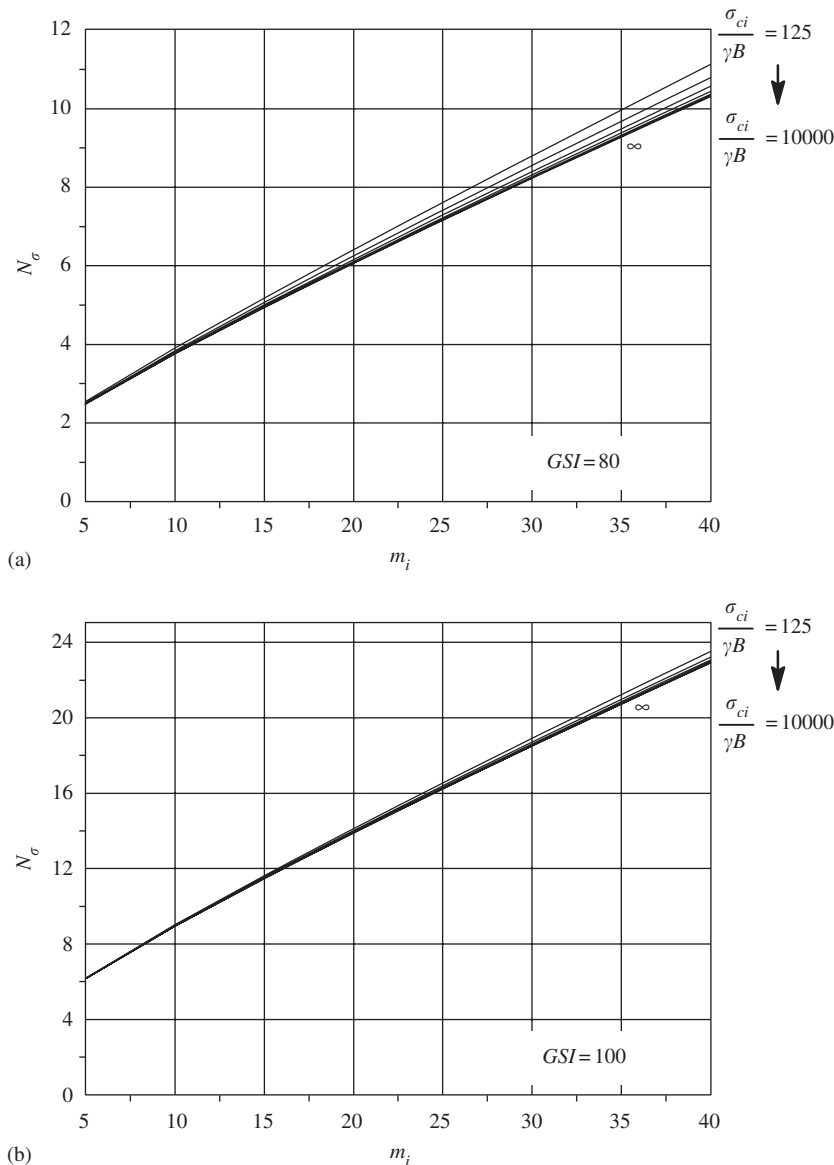


Fig. 12. Average finite element limit analysis values of the bearing capacity factor N_{σ} .

γ is only likely to have a small effect on the bearing capacity factor N_σ .

The effect of the rock weight γ was found to decrease with increasing GSI . This is shown clearly in Figs. 9–12 where the lines represented by the ratio $\sigma_{ci}/\gamma B$ begin to converge towards the weightless case where $\sigma_{ci}/\gamma B = \infty$. At $GSI = 100$ (Fig. 12(b)), the ratio $\sigma_{ci}/\gamma B$ has very little influence on the bearing capacity and the observed velocity fields are almost identical regardless of the $\sigma_{ci}/\gamma B$ value (see Fig. 15(b)). This implies that the rock mass strength behaviour is very much dominated by cohesion and is almost independent of the mean normal stress. In addition, the effect of rock weight also decreases with intact rock

strength σ_{ci} for a given GSI as illustrated in Fig. 13. For example, referring to Fig. 13, for a ratio of $\sigma_{ci}/\gamma B = 125$, $m_i = 10$ and $GSI = 10$, the bearing capacity for a ponderable rock mass is approximately 2.4 times that of a weightless rock mass. However, for $GSI = 40$ the ratio of $N_\sigma/N_{\sigma 0}$ decreases to around 1.3.

Several of the observed upper bound velocity plots and zones of plastic yielding for ponderable rock masses are shown in Figs. 14 and 15. In general it is observed that the extent of the velocity field and zone of plastic yielding increases with m_i and $\sigma_{ci}/\gamma B$ for $GSI < 60$. For values of $GSI > 60$ (Fig. 15(b)) the ratio of $\sigma_{ci}/\gamma B$ and m_i have less effect on the observed failure mode and plastic zones.

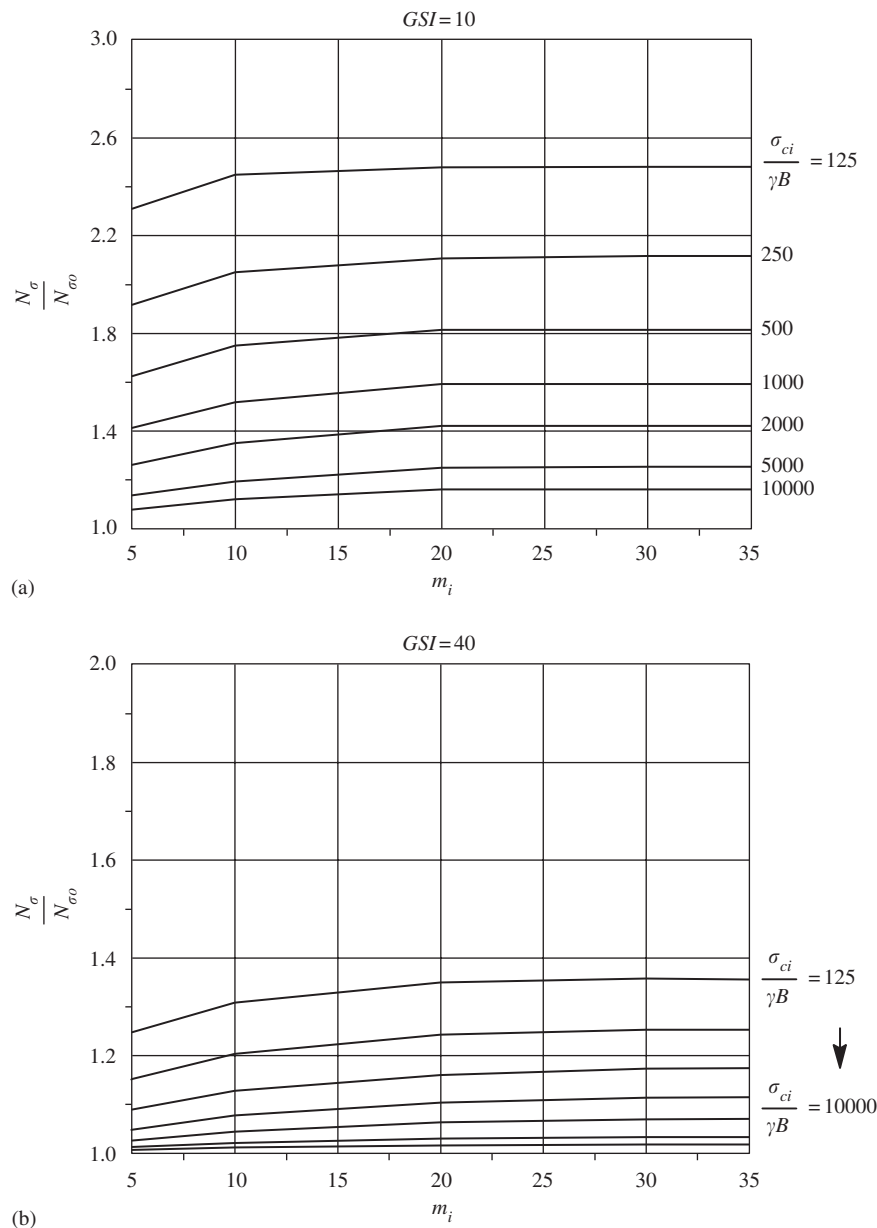


Fig. 13. Effect of soil weight and strength on ultimate bearing capacity.

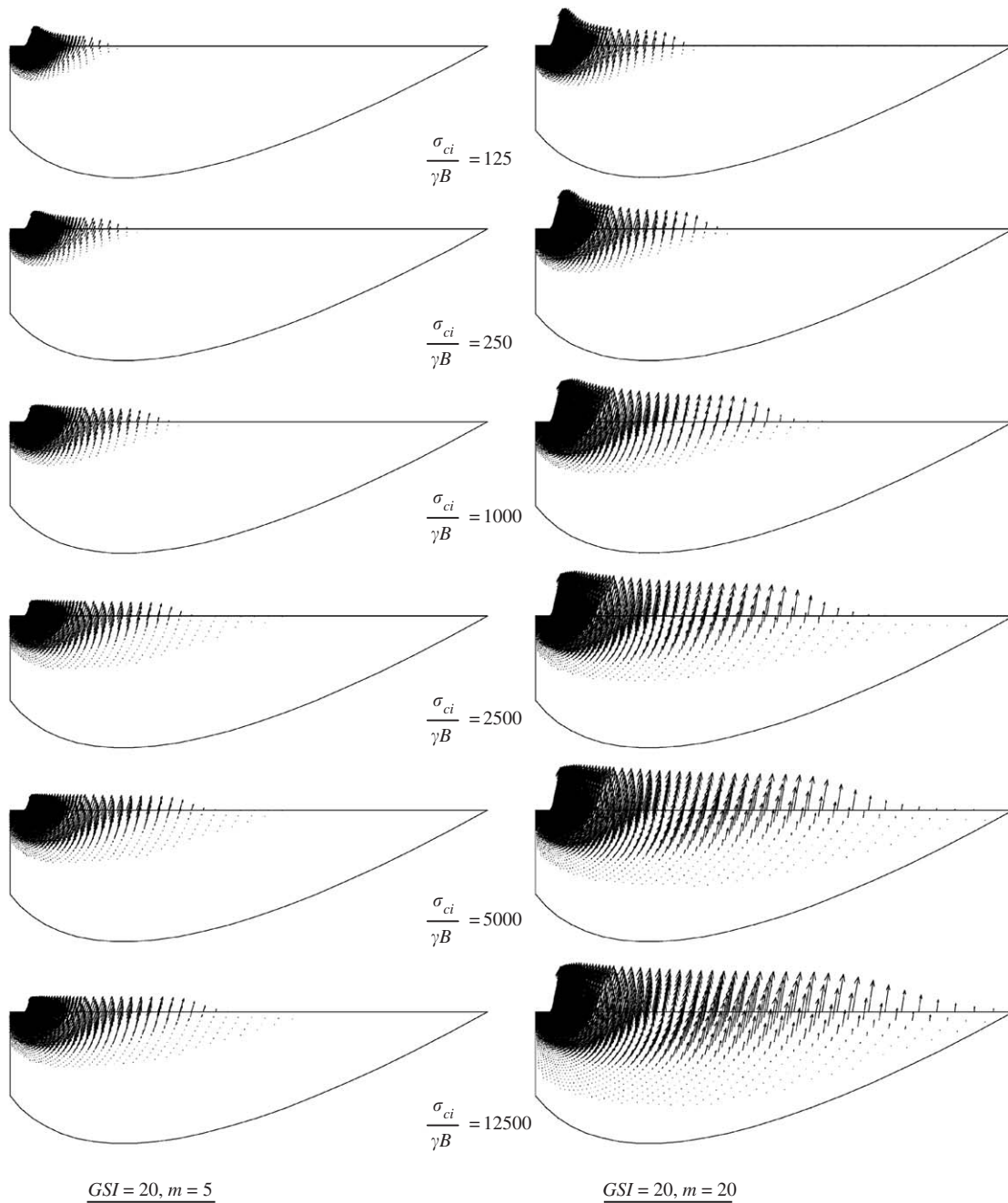


Fig. 14. Upper bound velocity fields and plastic zones for rock with weight.

6. Comparison with previous numerical studies

As a preliminary comparison, several limit analyses were performed for weightless rock masses using equivalent Mohr–Coulomb parameters as determined by Eqs. (16) and (15). Table 2 presents the results obtained for three different quality rock masses. The equivalent Mohr–Coulomb parameters were obtained over two separate ranges of the minor principal stress σ_3 ; namely, $0 < \sigma_3 < 0.25\sigma_{ci}$ and $0 < \sigma_3 < 0.75\sigma_{ci}$. This table, along with Fig. 16, indicates just how sensitive the interpreted values of c'

and ϕ' are to the value of σ'_{3max} . Indeed, the cohesion can vary by as much as 100% for each rock mass quality.

It should be stressed that using a linear failure envelope in place of the curved Hoek–Brown envelope will affect the predicted bearing capacity. To highlight this, finite element upper bound analyses were performed using the Hoek–Brown and equivalent Mohr–Coulomb material parameters in Table 2 and the ultimate bearing capacity results are shown in Table 3. It can be seen that, for both ranges of the minor principal stress σ_3 , the ultimate bearing capacity has been overestimated significantly (46–157%) when we

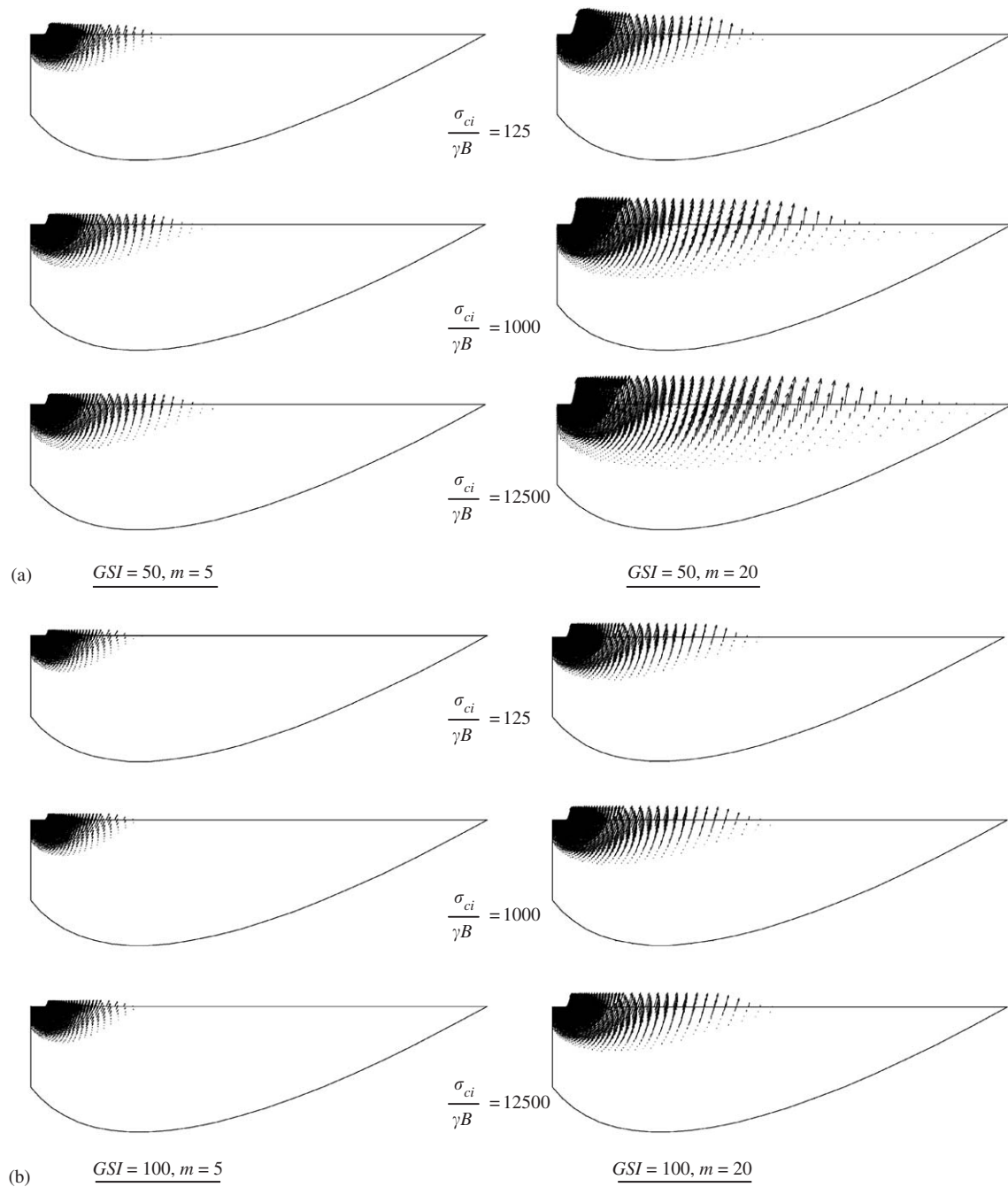


Fig. 15. Upper bound velocity fields and plastic zones for rock with weight.

Table 2
Determination of equivalent Mohr–Coulomb parameters for various quality rocks

Rock quality	σ_{ci}	m_i	GSI	$0 < \sigma_3 < 0.25\sigma_{ci}$		$0 < \sigma_3 < 0.75\sigma_{ci}$	
				c'	ϕ'	c'	ϕ'
Very poor	20	8	30	0.65	22.8	1.3	15.9
Average	80	12	50	4.2	32.1	8.55	23.4
Very good	150	25	75	14.1	45.8	28.6	36.6

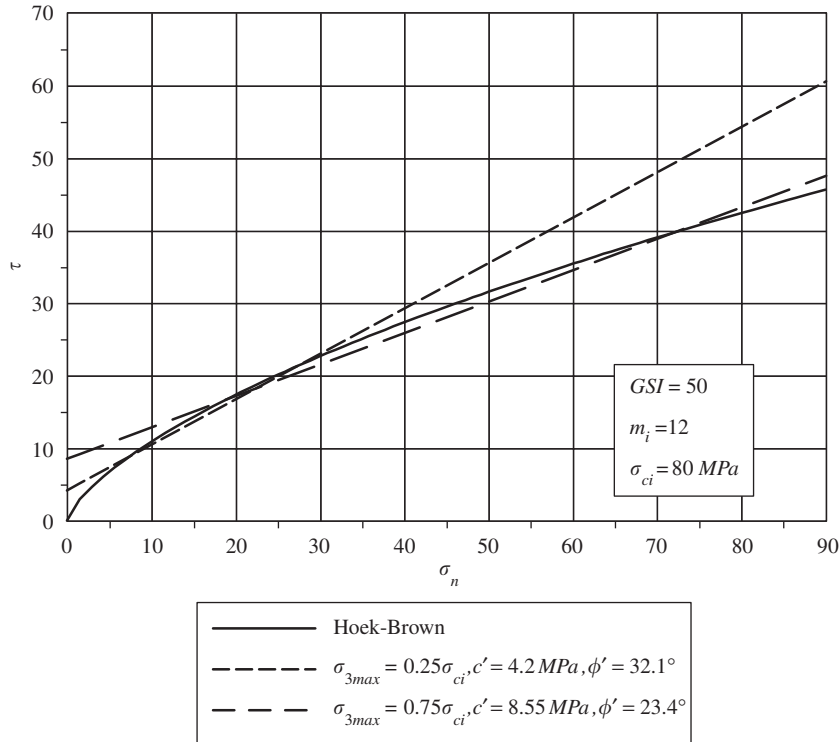


Fig. 16. Failure envelopes and equivalent Mohr–Coulomb parameters for average quality rocks.

Table 3
Comparison of ultimate bearing capacity using Hoek–Brown and equivalent Mohr–Coulomb material parameters for various quality rocks-weightless

Rock quality	q_u (MPa) Hoek–Brown	$0 < \sigma_3 < 0.25\sigma_{ci}$	$0 < \sigma_3 < 0.75\sigma_{ci}$	q_u (MPa) Serrano et al. [24]
		q_u (MPa) Mohr–Coulomb	q_u (MPa) Mohr–Coulomb	
Very poor	6.7	12.0 (+46%)	15.3 (+87%)	6.5 (–3%)
Average	98.5	156.4 (+59%)	161.0 (+63%)	94.4 (–4%)
Very good	886.0	2279.4 (+157%)	1614.6 (+82%)	870.4 (–1%)

adopt equivalent Mohr–Coulomb strength parameters. Although the inclusion of rock weight γ is likely to increase the ultimate values shown in Table 3 by up to 25%, the overall predictions will still be poor for these rock qualities. The only method for improving the comparison would be to re-analyse each problem until equivalent Mohr–Coulomb strength parameters c and ϕ are found such the ultimate bearing capacity matches those obtained from the Hoek–Brown criterion. Given that a comprehensive set of bearing capacity solutions is provided herein, there is little point in carrying out such analyses.

The lower bound results obtained from the method proposed Kulhaway and Carter [20] (Eqs. (18) and (19)) are compared to the average finite element upper and lower bounds in Table 1. Due to the very simple lower bound stress field that is assumed, their estimates of the bearing capacity factor N_{co} are rather conservative and are typically 30–80% below the average finite element limit analysis results.

To make a direct comparison between the finite element limit analysis results and the results obtained by Serrano et al. [24] for weightless rock, Eq. (20) can be re-written as

$$N_{\sigma 0(\text{Serrano})} = \frac{q_u}{\sigma_{ci}} = \frac{\beta_b(N_\beta - \zeta_n)}{\sigma_{ci}}, \tag{21}$$

where $N_{\sigma 0(\text{Serrano})}$ can be compared directly to the value of $N_\sigma = N_{\sigma 0}$ in Eq. (17).

The bearing capacity factor obtained from Eq. (21) is compared to the average limit analysis results in Table 1. The method proposed by Serrano et al. [24] provides estimates of the bearing capacity factor $N_{\sigma 0}$ that are remarkably close to the finite element results and in most cases within a few percent. This is also confirmed by the comparison in Table 3 for several broad rock types. The only exception to this observation occurs for a small class of very poor quality rocks with $GSI \leq 10$, where the method of Serrano et al. is more conservative and underestimates the bearing capacity factor by up to 35%.

7. Conclusions

The bearing capacity of a surface strip footing resting on a rock mass whose strength can be described by the generalised Hoek–Brown failure criterion has been investigated. Using powerful new formulations of the upper and lower bound limit theorems, rigorous bounds on the bearing capacity for a wide range of material properties have been obtained. The results have been presented in terms of a bearing capacity factor N_σ in graphical form to facilitate their use in solving practical design problems.

The following conclusions can be made based on the limit analysis results:

- (a) The computed upper and lower bound estimates of the bearing capacity factor N_σ , for either weightless or ponderable rock foundations, were found to be within 5% of each other. This indicates that, for practical design purposes, the true collapse load has been bracketed to within $\pm 2.5\%$ or better.
- (b) The effect of ignoring rock weight can lead to a very conservative estimate of the ultimate bearing capacity. This is particularly the case for poorer quality rock types with GSI values less than approximately 30, where the ultimate bearing capacity can be as much as 60% below the actual capacity when rock weight is included.
- (c) Estimating the ultimate bearing capacity of a rock mass using equivalent Mohr–Coulomb parameters was found to significantly overestimate the bearing capacity. This overestimate was found to be as high as 157% for very good quality rock masses.
- (d) Existing numerical solutions for weightless rock masses are generally conservative and can differ from the bound solutions by up to 80%.

References

- [1] Lyamin AV, Sloan SW. Lower bound limit analysis using non-linear programming. *Int J Numer Methods Eng* 2002;55(5):573–611.
- [2] Lyamin AV, Sloan SW. Upper bound limit analysis using linear finite elements and non-linear programming. *Int J Numer Anal Methods Geomech* 2002;26(2):181–216.
- [3] Sutcliffe D, Yu HS, Sloan SW. Lower bound solutions for bearing capacity of jointed rock. *Comput Geotech* 2004;31(1):23–36.
- [4] Zheng X, Booker JR, Carter JP. Limit analysis of the bearing capacity of fissured materials. *Int J Solids Struct* 2000;37(8):1211–43.
- [5] Sloan SW. Lower bound limit analysis using finite elements and linear programming. *Int J Numer Anal Methods Geomech* 1988;12(1):61–7.
- [6] Sloan SW, Kleeman PW. Upper bound limit analysis using discontinuous velocity fields. *Comput Methods Appl Mech Eng* 1995;127(1–4):293–314.
- [7] Hoek E, Carranza-Torres C, Corkum B. Hoek–Brown failure criterion—2002 edition. In: *Proceedings of the North American rock mechanics society meeting in Toronto*; 2002.
- [8] Hoek E, Brown ET. Empirical strength criterion for rock masses. *J Geotech Eng Div ASCE* 1980;106(9):1013–35.
- [9] Mostyn G, Douglas K. Strength of intact rock and rock masses. In: *Proceedings of the international conference on geotechnical and geological engineering, Melbourne, Australia, vol. 1*. Lancaster: Technomic Publishing Co. Inc., 19–24 November 2000. p. 1389–421.
- [10] Hoek E. Strength of jointed rock masses. *Geotechnique* 1983;33(3):187–223.
- [11] Serrano A, Olalla C. Ultimate bearing capacity of an anisotropic discontinuous rock mass, part I: basic modes of failure. *Int J Rock Mech Min Sci* 1998;35(3):301–24.
- [12] Hoek E. A brief history of the development of the Hoek–Brown failure criterion. (<http://www.rocksience.com>). 2004.
- [13] Bieniawski ZT. Rock mass classification in rock engineering. In: Bieniawski ZT, editor. *Exploration for rock engineering, proceedings of the symposium, vol. 1*. Cape Town: Balkema; 1976. p. 97–106.
- [14] Barton N. Some new Q-value correlations to assist in site characterisation and tunnel design. *Int J Rock Mech Min Sci* 2002;39(2):185–216.
- [15] Abbo AJ, Sloan SW. A smooth hyperbolic approximation to the Mohr–Coulomb yield criterion. *Comput Struct* 1995;54(3):427–41.
- [16] Hoek E. Practical rock engineering: an ongoing set of notes. (<http://www.rocksience.com>). 2002.
- [17] Hoek E, Brown ET. Practical estimates of rock mass strength. *Int J Rock Mech Min Sci* 1997;34(8):1165–86.
- [18] Serrano A, Olalla C. Ultimate bearing capacity of an anisotropic discontinuous rock mass, part II: determination procedure. *Int J Rock Mech Min Sci* 1998;35(3):325–48.
- [19] Carter JP, Kulhawy FH. Analysis and design of drilled shaft foundations socketed into rock. Rep. EL-5918. Palo Alto, CA: Electric Power Research Institute; 1988.
- [20] Kulhawy FH, Carter JP. Settlement and bearing capacity of foundations on rock masses and socketed foundations in rock masses. In: Bell FG, editor. *Engineering in rock masses*. Oxford, UK: Butterworth-Heinemann; 1992. p. 231–45.
- [21] AASHTO. Standard specifications for highway bridges. Washington, DC: American Association of State Highway and Transport Officials; 1997.
- [22] Serrano A, Olalla C. Ultimate bearing capacity of rock masses. *Int J Rock Mech Min Sci Geomech Abstr* 1994;31(2):93–106.
- [23] Serrano A, Olalla C. Allowable bearing capacity in rock foundations, using a non-linear failure criterion. *Int J Rock Mech Min Sci* 1996;33(4):327–45.
- [24] Serrano A, Olalla C, Gonzalez J. Ultimate bearing capacity of rock masses based on the modified Hoek–Brown criterion. *Int J Rock Mech Min Sci* 2000;37(6):1013–8.
- [25] Sokolovskii VV. *Statics of granular media*. London, UK: Pergamon Press; 1965.
- [26] Hoek E, Wood D, Shah S. A modified Hoek–Brown failure criterion for jointed rock masses. In: *Eurock '92*; 1992. p. 209–13.
- [27] Serrano A, Olalla C. Ultimate bearing capacity at the tip of a pile in rock; theory (part I). *Int J Rock Mech Min Sci* 2002;39(7):833–46.
- [28] Serrano A, Olalla C. Ultimate bearing capacity at the tip of a pile in rock—part 2: application. *Int J Rock Mech Min Sci* 2002;39(7):847–66.
- [29] Yang X, Yin J-H, Li L. Influence of a non-linear failure criterion on the bearing capacity of a strip footing resting on rock mass using a lower bound approach. *Can Geotech J* 2003;40(3):702–7.